Kang, K., Schenkeveld, W. D. C., Biswakarma, J., Borowski, S. C., Hug, S. J., Hering, J. G., & Kraemer, S. M. (2019). Low Fe(II) concentrations catalyze the dissolution of various Fe(III) (hydr)oxide minerals in the presence of diverse ligands and over a broad pH range. Environmental Science and Technology, 53(1), 98-107.
https://doi.org/10.1021/acs.est.8b03909

Low Fe(II) concentrations catalyze the dissolution of various Fe(III) (hydr)oxide minerals in the presence of diverse ligands and over a broad pH range

Kyounglim Kang[a], Walter D.C. Schenkeveld[a*†], Jagannath Biswakarma[b,c], Susan C. Borowski[b‡], Stephan J. Hug[b], Janet G. Hering[b,c,d], Stephan M. Kraemer[a*].

[a] Department of Environmental Geosciences, University of Vienna, Althanstrasse 14(UZA II) 1090 Vienna, Austria.

[b] EAWAG, Swiss Federal Institute of Aquatic Science and Technology, Ueberlandstr. 133, CH-8600, Dübendorf, Switzerland

[c] Swiss Federal Institute of Technology (ETH) Zürich, IBP, CH-8092 Zürich, Switzerland

[d] Swiss Federal Institute of Technology Lausanne (EPFL), ENAC, CH-1015 Lausanne, Switzerland

† Current address: W.D.C. Schenkeveld, Copernicus Institute, Faculty of Geosciences, Utrecht University, Princetonlaan 8A, 3584 CB Utrecht, the Netherlands

‡Current address: S.C. Borowski, Virginia Military Institute, Lexington, VA 24450, USA.

*E-mail: w.d.c.schenkeveld@uu.nl; stephan.kraemer@univie.ac.at

4946 Words

3 Figures

1 Table

Abstract

Dissolution of Fe(III) (hydr)oxide minerals by siderophores (i.e. Fe-specific, biogenic ligands) is an important step in Fe acquisition in environments where Fe availability is low. The observed co-exudation of reductants and ligands has raised the question of how redox reactions might affect ligand-controlled (hydr)oxide dissolution and Fe acquisition. We examined this effect in batch dissolution experiments using two structurally distinct ligands (desferrioxamine B (DFOB) and N,N′-di(2-hydroxybenzyl)ethylene-diamine-N,N′-diacetic acid (HBED)) and four Fe(III) (hydr)oxide minerals (lepidocrocite, 2-line ferrihydrite, goethite and hematite) over an environmentally-relevant pH range (4 - 8.5). The experiments were conducted under anaerobic conditions with varying concentrations of (adsorbed) Fe(II) as the reductant. We observed a catalytic effect of Fe(II) on ligand-controlled dissolution even at sub-micromolar Fe(II) concentrations with up to a 13-fold increase in dissolution rate. The effect was larger for HBED than for DFOB. It was observed for all four Fe(III) (hydr)oxide minerals, but it was most pronounced for goethite in the presence of HBED. It was observed over the entire pH range with the largest effect at pH 7 and 8.5, where Fe deficiency typically occurs. The occurrence of this catalytic effect over a range of environmentally relevant conditions and at very low Fe(II) concentrations suggests that redox-catalysed, ligand-controlled dissolution may be significant in biological Fe acquisition and in redox transition zones.

Keywords:

Ligand-controlled dissolution, reductive dissolution, Fe(II), catalytic effect, synergism, Fe acquisition, pH, Fe(hydr)oxides, DFOB, HBED, electron transfer, atom exchange

Introduction

Dissolution of Fe(III) (hydr)oxide minerals is an important process in the natural Fe cycle and for biological Fe acquisition. Despite its crustal abundance, the bioavailability of Fe is often insufficient to meet the requirements of organisms due to the poor solubility and slow dissolution kinetics of Fe(III) (hydr)oxide minerals at circum-neutral pH[1]. This exerts a selective pressure favouring organisms that have evolved highly efficient Fe acquisition strategies. Secretion of protons, reductants and ligands allows proton-promoted, reductive, and ligand-controlled dissolution, all of which involve surface-controlled dissolution mechanisms [2]. Proton-promoted Fe(III) (hydr)oxide dissolution is very slow in the neutral to alkaline pH range[3]; the required acidic conditions are difficult to generate in well-buffered (e.g. carbonatic) systems. In reductive Fe(III) (hydr)oxide dissolution, structural Fe(III) is reduced to Fe(II) at the mineral surface. Because Fe(II) is kinetically more labile than Fe(III), detachment is facilitated, leading to increased dissolution rates. The greater solubility of Fe(II) minerals also allows for higher concentrations of dissolved Fe in equilibrium with the solid. However, in the presence of oxygen and particularly at circum-neutral pH, reduced Fe(II) is quickly re-oxidized to Fe(III) by a surface-catalyzed process.[4, 5] This fast re-oxidation inhibits the mobilization of Fe, unless ligands are present that either stabilize the Fe(II) redox state [6] or form Fe(III) complexes in solution. Ligand-controlled Fe(III) (hydr)oxide dissolution involves the formation of ligand-surface complexes that weaken the bond between the Fe(III) participating in the surface complex and the mineral matrix, facilitating detachment.[1, 7-12] Both biogenic ligands (e.g. desferrioxamine B (DFOB)) and synthetic ligands (e.g. *N,N*′-di(2-hydroxybenzyl)ethylene-diamine-*N,N*′-diacetic acid

(HBED)) can enhance Fe bioavailability [13, 14]. However, ligand-controlled dissolution is slow compared to reductive dissolution.[15,16]

Synergistic Fe mobilization by ligands in the presence of reductants or Fe(II) at low pH was shown in the 1980s, falsifying previous assumptions regarding the additivity of reductive and ligand-controlled dissolution rates.[17] Observation of co-exudation of reductants and ligands by microorganisms and plants [18, 19] suggested that synergistic effects of reductants and ligands might also occur in the neutral and alkaline pH range. Such effects were recently demonstrated at circumneutral pH in oxic and anoxic goethite suspensions[20], as well is in oxic soil suspensions[21].

Banwart et al. suggested a mechanism for the catalysis of ligand-controlled dissolution where adsorbed Fe(II)-ligand complexes served as reductant and accelerated the rate-determining detachment of Fe from the surface [17, 22]. Specifically, they proposed that adsorption leads to the formation of ternary surface complexes where the bridging ligand (in their case oxalate) transfers an electron from the adsorbed Fe(II) to a structural Fe(III) atom at the mineral surface [17, 22]. Subsequently, desorption of the adsorbed Fe(III)-ligand surface complex and rate-determining detachment of Fe(II) from the surface contribute to the net dissolution reaction. This mechanism does not involve electron transfer through the mineral structure. An alternative mechanism has been proposed on the basis of previous observations that adsorption of Fe(II) to Fe(III) (hydr)oxide surfaces induces electron transfer through the mineral [23-27]. If this electron transfer destabilizes the coordination environment of Fe at the mineral surface, the rate of ligand-controlled dissolution could be enhanced as has been suggested for observations of synergistic effects of ligands and reductants on goethite dissolution[20].

The aim of this study was to explore the potential catalytic effect of Fe(II) in ligand-controlled Fe(III) (hydr)oxide dissolution for Fe acquisition strategies under a variety of environmental conditions. In this context, significant knowledge gaps exist regarding the specificity of the effect with respect to mineral structure, ligand structure and pH. Furthermore, the development of rate laws for the quantification of these effects is lacking. To close these gaps and to provide the groundwork for further explorations of the underlying mechanisms, we conducted a series of dissolution experiments under anoxic conditions in which the added Fe(II) concentration, the ligand, the mineral and the pH were varied. Our results demonstrate the broad relevance of this effect beyond specific mineral structures, ligand structures and in a broad pH range. Our observation of significant catalytic effects even at very low transient Fe(II) concentrations suggest that this mechanism may be important in environments where nutrient limitation occurs, including oxic environments at circumneutral pH where Fe(II) produced by thermal or photochemical redox reactions is rapidly reoxidized.

Materials and Methods

Five Fe(III) (hydr)oxide minerals were used: goethite-1 (α-FeOOH, specific surface area (SSA): 105 $m^2\ g^{-1}$), goethite-2 (α-FeOOH, SSA: 32 $m^2\ g^{-1}$), lepidocrocite (γ-FeOOH, SSA: 70 $m^2\ g^{-1}$), hematite (α-Fe_2O_3, SSA: 22 $m^2\ g^{-1}$) and 2-line ferrihydrite. Goethite-1 was synthesized according to Hiemstra et al.[28], hematite was synthesized by a sol gel method according to Sugimoto et al.[29], and the other minerals were synthesized according to the standard synthesis methods in Schwertmann and Cornell (2008)[30], as described in detail in Mørup et al.[31] and Schwertmann et al.[32], respectively. The purity and crystal structure of each Fe(III) (hydr)oxide were confirmed by X-ray powder diffraction (XRD, Huber 5042 four-circle diffractometer) (Figure S7). Mineral transformations during our experiments have not been assessed. Based on previous studies with such low examined Fe(II) concentrations, mineral transformations of Fe(III) (hydr)oxide minerals are unlikely to occur on our experimental time-scales[33, 34]. Specific surface areas were determined by a multipoint N_2-BET adsorption method (Quantachrome Nava 2000). We assume that the BET surface area is an appropriate predictor for the ligand-accessible surface area except for 2-line ferrihydrite where this assumption fails [35, 36].

Ligands and pH buffers were obtained from commercial sources and used as received. DFOB (a trishydroxamate) and HBED (containing amine, phenol and carboxyl groups) have been used as ligands. These ligands have a high affinity for Fe(III) ($\log ß_{11}$ = 33.0 and 39.0 for DFOB and HBED, respectively (I=0)). The examined ligands have been investigated intensively regarding their structure, solution speciation and reactivity [20]. Further information on the chemicals is available in the Supporting Information (Table S1). Ultrapure water (resistivity > 18.2 MΩ·cm, TOC < 2 ppb, Milli-Q, Millipore) was used to prepare all solutions and suspensions.

The pH of solutions and suspensions was monitored throughout the experiments with a pH meter (Orion 3 star, Thermo). Total dissolved Fe concentrations were measured by inductively coupled plasma mass spectrometry (ICP-MS, Agilent-7700; limit of quantification: 0.8 µg L^{-1} Fe

(0.014 µM)). The total DFOB and HBED solution concentrations were determined by measuring light absorbance of the corresponding Fe(III) complexes using a UV-vis spectrophotometer (Varian Cary 50) after addition of an Fe(III) solution to ensure complete complex formation. Absorbance was measured at the respective absorbance maxima of Fe(III)-DFOB (428 nm; ε = ~2820 M^{-1} cm^{-1}) and Fe(III)-HBED (493.1 nm; ε =~3440 M^{-1} cm^{-1}). Redox speciation of the complexed Fe in solution was not examined.

Batch dissolution experiments

The influence of the Fe(II) concentration on Fe(II) catalysed ligand-controlled dissolution rates was examined in lepidocrocite suspensions (0.1 g L^{-1}) by varying the Fe(II) concentration from 0 to 5 µM and subsequently adding a fixed ligand concentration. Under oxic conditions or in redox transition zones where Fe(III) (hydr)oxide minerals may be found, Fe(II) concentrations are typically low and often transient. Therefore we explore a low Fe(II) concentration range. The effect of pH on the catalytic effect of Fe(II) was examined by fixing the pH of lepidocrocite suspensions (0.1 g L^{-1}) with buffers at pH values of 4, 6, 7 and 8.5 and applying treatments containing 5 µM Fe(II), 20 µM DFOB or both. The order of addition of Fe(II) and DFOB in combined treatments was varied (either Fe(II) and DFOB added at the same time, or Fe(II) added 20 minutes before DFOB, where the DFOB addition was considered t=0) in order to test the effect of adsorption equilibration on dissolution rates. To assess whether Fe(II) was initially complexed by DFOB in treatments with simultaneous Fe(II) and DFOB application, the aqueous equilibrium speciation of 5 µM Fe(II) in the presence of 20 µM DFOB (in absence of surfaces) was modelled as a function of pH with PhreeqC using the Minteq v4 database[37] supplemented with protonation and complexation constants for DFOB presented in Kim et al[38]. The effect of the type of Fe(III) (hydr)oxide mineral on the catalytic effect of Fe(II) was examined in 0.1 g L^{-1} suspensions of lepidocrocite, goethite-1, goethite-2, hematite and 2-line ferrihydrite, to which a fixed ligand concentration or Fe(II) or both (adding Fe(II) first) were added. 1 µM Fe(II) was added in HBED treatments at pH 6 and 2 µM Fe(II) in DFOB treatments at pH 7.

Dissolution experiments were carried out in an anaerobic chamber (mBRAUN, unilab 7185) under a nitrogen atmosphere at constant temperature (20 ± 1 °C). The O_2 concentration was monitored and controlled to less than 1 ppm. All water used had been pre-boiled for more than 1 h and was purged with N_2 while cooling down before introduction into the anaerobic chamber. For introduction of (N_2-purged) liquids and solid materials into the chamber, the atmosphere in the antechamber was exchanged with N_2 gas at least 5 times. The batch reactors (LDPE, 100 ml) were wrapped in aluminium foil to prevent potential photo-reduction. All Fe(III) (hydr)oxide suspensions were thoroughly mixed with a magnetic stirrer and a Teflon-coated stirring bar. NaCl was applied as background electrolyte to a final concentration of 0.01 M. The effect of the electrolyte and ionic strength was not further explored in this work. The pH was buffered with 0.005 M of either PIPPS (pH 4 and pH 8.5), MES (pH 6), or MOPS (pH 7). Batch dissolution and adsorption experiments were conducted at the same buffer concentration so that potential effects from buffers on ligand and Fe(II) adsorption[39] could be accounted for in parameterizing rate law equations of surface-controlled dissolution reactions. The pH was set by adding HCl or NaOH, and remained constant at the set pH values (ΔpH = ±0.05) throughout the experiments. The Fe(III) (hydr)oxide suspensions containing buffer and electrolyte were equilibrated overnight in the anaerobic chamber prior to addition of Fe(II) and ligand at 90 % of final suspension volume. The final volume (and suspension concentration) was reached after the addition of Fe(II) and ligand stock solutions as described below. Experimental solutions were prepared under anaerobic conditions. Except for HBED, all chemicals readily dissolved in deoxygenated ultrapure water. HBED was dissolved by adding 0.1 M of NaOH solution to prepare the 700 µM stock solution. The stock solutions were prepared at a pH close to the experimental pH. Fe(II) was added to the pre-equilibrated solutions 20 minutes prior to the ligand. t=0 corresponds with the moment of ligand addition. Samples were collected periodically for a period of 24 h, were filtered through 0.1 μm PVDF syringe filters (Merck, Millipore, catalogue no. SLVV033RS), and were acidified with trace metal grade HNO_3 for analysis of the dissolved Fe concentration by ICP-MS. Dissolution experiments were carried out in duplicates. Mineral dissolution did not exceed 2% of the bulk in any experiment.

Dissolution rates were calculated from the slopes of linear regression lines of the dissolved Fe concentration over time for the data points over which the increase of dissolved Fe(III) was linear; this interval was from 0.5 to 2.0 h for lepidocrocite at pH 6 but longer intervals were used under other conditions (Table S2). The rates are usually normalized to mineral surface area except for 2-line ferrihydrite dissolution rates which are presented as mass normalized rates because ligand-accessible specific surface area cannot be determined by BET analysis.

For ligand-controlled dissolution far from the equilibrium solubility of the mineral, steady-state dissolution can be expressed in a rate law that relates the dissolution rate to the adsorbed ligand concentration[40]:

$$R_{net} = k\,[\mathrm{L}]_{\mathrm{ads}} \qquad (1)$$

where R_{net} (pmol s^{-1} m^{-2}) is the net dissolution rate, k (s^{-1}) is a pseudo-first-order dissolution rate coefficient and $[\mathrm{L}]_{\mathrm{ads}}$ (µmol m^{-2}) is the adsorbed ligand concentration.

Assuming that the presence of adsorbed Fe(II) catalyzes ligand-controlled dissolution, we hypothesize that the effect on the rate coefficient can be expressed as:

$$k = k_{\mathrm{L},} + k_{Fe(II)}[\mathrm{Fe(II)}]_{\mathrm{ads}} \qquad (2)$$

where k_{L} is the rate coefficient of ligand-controlled dissolution and $k_{Fe(II)}$ is the rate coefficient associated with the effect of Fe(II) on ligand-controlled dissolution. In the absence of Fe(II), k equals to $\mathrm{k_L}$ and in the presence of Fe(II) k equals to $k_{\mathrm{L},} + k_{Fe(II)}[\mathrm{Fe(II)}]_{\mathrm{ads}}$.The overall rate law becomes:

$$R_{net} = k_{\mathrm{L},}\,[\mathrm{L}]_{\mathrm{ads}} + \mathrm{k}_{\mathrm{Fe(II)}}[\mathrm{Fe(II)}]_{\mathrm{ads}}\,[\mathrm{L}]_{\mathrm{ads}} = R_L + R_{cat} \qquad (3)$$

Where $\mathrm{R_L}$ is the ligand-controlled dissolution rate and $\mathrm{R_{cat}}$ is the rate enhancement due to Fe(II) catalysis. The hypothesized catalytic effect (CE) of Fe(II) would correspond to $\mathrm{R_{net}/R_L}$ (i.e., the ratio of the net rate of dissolution in the presence of the ligand and Fe(II), $\mathrm{R_{net}}$, to the rate of dissolution in the presence of the ligand and the absence of Fe(II), $\mathrm{R_L}$). This rate law formulation is comparable to that of Suter et al., 1988[41], who proposed independent (additive) rates of ligand-controlled dissolution and reductive dissolution by an Fe(II)-ligand complex at Fe oxide surfaces.

Adsorption experiments

Adsorption isotherms were determined for sorption of Fe(II), Fe(III)DFOB, Fe(III)HBED, DFOB, HBED to Fe(III) (hydr)oxide minerals at pH 6 with 0.01 M NaCl as electrolyte. Additionally, Fe(II), adsorption to lepidocrocite was examined as a function of pH. For the ligands and Fe(III)-ligand complexes adsorption isotherms were determined in the presence and absence of 1 µM Fe(II) to examine the influence of Fe(II) on their adsorption behaviour. Experimental determination of Fe(II) adsorption in the presence of ligands was not feasible due to the fast Fe(III) mobilization by the ligands and the strong interference of the Fe-complexes in the spectrophotometric determination of Fe(II) concentrations.

All adsorption experiments were carried out in an anaerobic tent under a N_2-atmosphere (O_2 concentration < 1 ppm, Coy Laboratory) at 20 ±1 °C. Reactors (Polypropylene, 15 mL) were completely mixed and pre-equilibrated overnight in an end-over-end shaker. Solids concentrations of 2.5 g L^{-1} at pH 4 and 6, and 0.5 g L^{-1} at pH 7 and 8.5 were used. For Fe(II) adsorption experiments, total Fe(II) concentrations of 0.5, 1, 5, 10, 20, 50, 100 and 250 µM were applied. After a reaction time of 0.5 h, samples were filtered (0.1 μm) and the filtrate was analyzed for the dissolved Fe concentration. To investigate the adsorption of ligands and Fe(III)-ligand complexes in the presence and absence of Fe(II), total ligand or complex concentrations of 1, 2, 5, 10, 20 and 50 µM were added to a suspension containing no Fe(II) or 1 µM Fe(II). Fe(II) was added 20 minutes before Fe(III)-ligand addition. Adsorption of complexes was examined after a reaction time of 0.5 h; the remaining concentration in solution was analysed by UV-vis photospectrometry. Ligand adsorption was examined after only 1 minute reaction time in order to minimize the formation of Fe chelate complexes during the adsorption experiments. Fe-ligand complexes accounted for less than 1.5% of the amount of ligand applied, except in the treatment with HBED and lepidocrocite, in which they accounted for up to 10%. For determining the adsorption isotherms of HBED, Fe(III)HBED adsorption was neglected, as it was shown to be very small under the experimental conditions. After interaction, the samples were filtered (0.1 µm). A subsample was analyzed by photospectrometry for the total Fe concentration mobilized by the ligand. To another subsample Fe(III) was added in a small excess over the ligand concentration to have all ligand form Fe chelates complexes. Excess Fe was allowed to precipitate overnight. The following day the subsample was filtered (0.1 µm) to remove Fe(III) precipitates and the sample was analyzed by UV-vis photospectrometry. All adsorption experiments were carried out in duplicates.

Results and Discussion

Influence of Fe(II) concentration on the rate of ligand-controlled dissolution of lepidocrocite

Results from lepidocrocite dissolution experiments with 20 µM DFOB or 17.6 µM HBED and various concentrations of Fe(II) at pH 6 are presented in Figure 1a and Figure 1c, respectively.

In a control treatment with 5 μM Fe(II), but without any ligand, the dissolved Fe concentration, $[Fe]_{diss}$ remained constant at approximately 2.0 μM, which can be attributed to adsorption. In experiments with added ligand but without added Fe(II), $[Fe]_{diss}$ increased linearly over time. With both added ligand and Fe(II), varying patterns in $[Fe]_{diss}$ over time were observed depending on the ligand and the amount of Fe(II) added.

With DFOB, $[Fe]_{diss}$ increased almost linearly over the entire course of the experiment (Figure 1a). Even with 5 μM added Fe(II), $[Fe]_{diss}$ at 9 h was still less than the expected maximum value. The maximum value would correspond to Fe(III) as 1:1 DFOB complex (20 μM) plus dissolved Fe(II). The dissolved Fe(II) concentration corresponds to the added Fe(II) concentration minus adsorbed Fe(II) concentration. The affinity of DFOB for Fe(II) is limited and thermodynamic calculations indicate that at pH 6 (in absence of reactive surfaces) less than 1% of 5 μM Fe(II) will be complexed in the presence of 20 μM DFOB (Table S3). This implies that the impact of DFOB on Fe(II) speciation under these experimental conditions is marginal. In the treatment with 5 μM Fe(II) and DFOB, the first measurement of $[Fe]_{diss}$ (at t = 0.5 h) corresponded roughly to the concentration of added Fe(II), suggesting the Fe adsorbed before addition of the ligand was rapidly released back into solution, possibly as Fe(III), when the ligand was added at t = 0 h. A similar observation was made in isotopic exchange experiments with a different ligand (EDTA), where ^{57}Fe added as ^{57}Fe(II) to lepidocrocite at pH 6.0 was rapidly released back into solution upon addition of EDTA, although release of ^{56}Fe also occured[42].

With the ligand HBED, the maximum expected value of $[Fe]_{diss}$ was observed at the first time point (t = 0.5 h) with 5 μM added Fe(II) and at the second time point (t = 1 h) with 1 μM added

Fe(II). A plateau in $[Fe]_{diss}$ was also observed at the expected maximum value at longer times (2, 3, and 5 h) for added Fe(II) concentrations of 0.8, 0.6 and 0.4 μM, respectively. Under these conditions, the values of $[Fe]_{diss}$ at t = 0.5 h were greater than the concentration of added Fe(II), suggesting that some rapid dissolution occurred before the first time point. We did not find reports of measured Fe(II)HBED stability constants and could therefore not calculate Fe(II) speciation under the experimental conditions. Dissolution rates (R_{net}) were extracted based on measured $[Fe]_{diss}$ from t = 0.5 to 2 h for added Fe(II) from 0 to 0.6 μM.

As shown in Figures 1 b and d, the observed dissolution rates increased linearly with adsorbed Fe(II) concentrations as measured in ligand-free systems (Fig. S1). A catalytic effect of Fe(II) was observed even at sub-micromolar levels, especially in the presence of HBED. The catalytic effect (R_{net}/R_L) was substantially stronger for HBED than for DFOB. The Fe(II) effect, as derived from the rate coefficients $k_{Fe(II)}$ in the presence of the two ligands, was 7 times larger for HBED ($k_{Fe(II)} = 1.8 \pm 0.6 \times 10^{-2}$ μmol^{-1} m^{2} s^{-1}) than for DFOB ($2.6 \pm 0.8 \times 10^{-3}$ μmol^{-1} m^{2} s^{-1}).

Dissolution rates (reported in Table S2) were calculated on a surface-normalized basis (described in Fig. S4) and rate coefficients were calculated using measured adsorbed ligand concentrations (Fig. S2). Ligand controlled dissolution in the absence of added Fe(II) was measured and corresponds to the y-intercepts of Figs. 1 b and d (Eqn. 1). With $[L]_{ads}$ of 1.7×10^{-1} μmol m^{-2} for both DFOB and HBED, the calculated rate coefficient for ligand controlled dissolution (k_L) is 1.7 times greater for HBED (4.2×10^{-4} s^{-1}) than for DFOB (2.5×10^{-4} s^{-1}).

In order to calculate the rate coefficients k_L and $k_{Fe(II)}$ from the observed rates, it was necessary to estimate the concentrations of the adsorbed ligands and Fe(II). This estimation assumed that ligand and Fe(II) adsorption were independent from each other. To test this assumption, HBED and DFOB adsorption at pH 6.0 were measured with 0 or 1 µM added Fe(II). The adsorption isotherms (Fig. S2) showed a small enhancement by Fe(II) in the case of HBED and a small inhibition by Fe(II) for DFOB. These contrasting effects can be attributed to an increase in positive surface charge due to Fe(II) adsorption, leading to increased electrostatic attraction between HBED ligands (dominant solution species at pH 6: H_3HBED^-) and the surface, but to increased repulsion between DFOB ligands (dominant solution species at pH 6: H_4DFOB^+) and the surface. Thus the values calculated for $k_{Fe(II)}$ may be slightly overestimated for HBED (if its adsorbed concentration was higher than the value used in the calculation) and slightly underestimated for DFOB. These effects, however, are expected to be minor in comparison with the effect of the ligand on the magnitude of $k_{Fe(II)}$. In the absence of detailed information on surface complex formation of DFOB and HBED, which is not available at the current stage, we cannot fully interpret the differences in reactivity between these ligands.

Influence of pH on Fe(II) catalysed ligand-controlled dissolution of lepidocrocite

In the absence of Fe(II), DFOB-controlled lepidocrocite dissolution rates increased by a factor of 2.9 over the pH range between pH 4.0 and 8.5 (Table S4). Borer et al.[43] found a somewhat smaller (1.6 fold) increase of DFOB-controlled lepidocrocite dissolution rates in the pH range from 3 to 8. They found that the increasing dissolution rates were correlated with increasing surface concentrations of DFOB while dissolution rate coefficients for DFOB were not pHdependent, suggesting that the surface speciation of adsorbed DFOB does not change over the pH range.

As shown in Figure 2 and Table S4, the addition of 5 µM Fe(II) had a clear effect on dissolved Fe concentrations over time. After 9 h the total dissolved Fe concentration amounted 14 - 19 µM Fe, depending on the pH. Comparing the results of dissolution experiments in the absence and the presence of Fe(II), it is important to note that elevated Fe concentrations in solution at the first time-point are partly due to the added Fe(II) concentration. For example, little Fe(II) sorption is expected at pH 4 due to electrostatic repulsion between the positively charged lepidocrocite surface and Fe(II) [44, 45]. Furthermore, equilibrium modelling results indicate that in absence of reactive surfaces, the extent to which 5 µM Fe(II) is complexed by 20 µM DFOB increases from less than 1 % at pH 6 to close to 100 % at pH 8.5 (Table S3). Therefore, sorption of Fe(II) and DFOB cannot be considered independent at pH >6. The degree to which Fe(II) is complexed in solution correlates with the difference in initial Fe mobilization (after 5 minutes) between the treatment in which Fe(II) and DFOB were applied simultaneously and the treatment in which Fe(II) was applied 20 minutes before the DFOB; at pH 6 there was no difference (Figure 2b), whereas at pH 8.5 the differences corresponded with the applied 5 µM of Fe(II) (Figure 2d). The order of Fe(II) and ligand addition had only a minor effect on apparent initial dissolution rates (5-30 minutes) and catalytic effects (Table S4). This suggests that after 5 min the order of addition did not influence the surface speciation including the precurcer of the rate controlling step.

The inhibition of Fe(II) sorption at pH 4 evidently also inhibited the catalytic effect (i.e., CE = 1.1) of Fe(II) on ligand-controlled dissolution. A 70-fold increase in Fe(II)$_{ads}$ surface concentration with increasing pH (measured in the absence of the ligand (Figure S1a-b)) lead to a 21-fold increase in dissolution rate from pH 4 to 7, and a CE of around 7 at pH 7 (Table S4). Between pH 7 and 8.5, the dissolution rates decreased by 50 %, possibly in part due to formation of Fe(II)-DFOB complexes in solution, inhibiting Fe(II) sorption as discussed above. Oxygen-independent oxidation of Fe(II) by a metal to ligand charge transfer as observed by Kim et al. 2010[38] may have also contributed to decreasing catalytic effects at elevated pH. Furthermore, the upper pH values (7 and 8.5) are close to the pristine point of zero charge of lepidocrocite; in this pH range changes in particle aggregation state may occur that could affect adsorption and the mineral dissolution rate[46, 47].

In the absence of adsorbed Fe(II), DFOB adsorption gradually increases with pH[43], but competitive adsorption of Fe(II) decreases DFOB adsorption (Figure S2a). The observation suggests that the interplay of these two effects leads to a maximum catalytic effect at pH 7.

Influence of the Fe(III) (hydr)oxide mineral on Fe(II) catalysed ligand-controlled dissolution

The effect of Fe(II) on the dissolution rates of various Fe(III) (hydr)oxides in the presence of DFOB or HBED is shown in Figure 3. Catalytic effects between 2.1 and 13 were observed for all Fe(III) (hydr)oxides (Figure 3 and Table 1). They were generally larger for HBED than for DFOB (except with 2-line ferrihydrite). Catalytic effects were not consistently correlated with mineral structure. The largest catalytic effect was observed for HBED-controlled goethite-2 dissolution, but in the presence of DFOB catalytic effects were larger for the less crystalline 2-line ferrihydrite and lepidocrocite compared to the more crystalline goethite and hematite. The presented rates (Table 1) are surface normalized. Application of the same total ligand concentration to a mineral with a lower SSA at the same suspension density can induce as shift along the adsorption isotherm potentially leading to a higher surface normalized dissolution rate. However, the rate order $k_{Fe(II)}$ provides a measure, independent of the adsorbed ligand concentration and specific surface area for comparing the catalytic effect among minerals. Therefore, rate coefficients (k_L and $k_{Fe(II)}$) for each Fe(III) (hydr)oxide (except 2-line ferrihydrite) were calculated according to rate equation 3 and 4. $HBED_{ads}$ was determined from Langmuir fits of HBED adsorption in the absence of Fe(II), $Fe(II)_{ads}$ was estimated from Langmuir fits of Fe(II) adsorption in the absence of a ligand. The effect of Fe(II) on HBED adsorption was shown to be small (Figure S2); the effect of HBED on Fe(II) adsorption is not known and may affect $k_{Fe(II)}$ calculations. The rate coefficients for ligand controlled dissolution k_{HBED} were of the same order of magnitude for all minerals except for hematite, where k_{HBED} was significantly smaller (Table 1 and Figure S6). Much larger variations were found for the rate coefficient $k_{Fe(II)}$ in the presence of HBED, with a maximum rate coefficient for goethite-2 and an almost two orders of magnitude lower rate coefficient for hematite. The large $k_{Fe(II)}$ for goethite-2 in the presence of HBED is consistent with the largest catalytic effect of HBED-controlled goethite-2 dissolution.

Environmental Implications of Fe-Catalysed Ligand-Controlled Dissolution

Fe(II) can play a pivotal role in biological Fe acquisition and natural Fe cycling of Fe(III) (hydr)oxide minerals. Our results demonstrate a catalytic effect of Fe(II) on ligand-controlled dissolution of Fe(III) (hydr)oxide minerals that scales linearly with the adsorbed concentration of Fe(II) under the experimental conditions. This effect was observed over the environmentally relevant pH range from 6 to 8.5, for two different ligands (HBED and DFOB) and for four Fe(III) (hydr)oxide minerals (lepidocrocite, 2-line ferrihydrite, hematite and goethite). Even at very low (sub-micromolar) concentrations, Fe(II) can strongly enhance the ligand-controlled dissolution rate of Fe(III) (hydr)oxide minerals. This is of particular relevance in the context of Fe acquisition strategies. Fe deficiency generally occurs under oxic conditions, where Fe(II) has a short residence time as a result of surface catalysed Fe(II) oxidation. Organisms that exude reductants for Fe acquisition may only generate low transient Fe(II) concentrations. Furthermore, we found that the catalytic effect of Fe(II) is not specific to a particular ligand. The ligands used in this investigation, DFOB (a biogenic siderophore) and HBED (a synthetic ligand), differ in charge, ligating groups and affinity for Fe(III). Therefore, it is probable that the observed catalytic effect may occur with a range of naturally occurring ligands. Its size was found to differ between the examined ligands. The catalytic effect of Fe(II) was observed for all examined Fe(III) (hydr)oxide minerals, which commonly occur in the environment, and the effect size depended on the mineral. The fact that the catalytic effect was largest around pH 7 is of particular environmental relevance as this is the pH range where solubility of Fe(III) (hydr)oxide minerals is lowest, Fe deficiency typically occurs and where the need for efficient Fe acquisition strategies is most pronounced. Research in microbial and plant physiology and ecology is needed to explore the significance of this effect for biological iron acquisition in natural systems. Similarly, further geochemical investigations are needed to address open questions with regard to the mechanism of the catalytic effect of Fe(II) on ligand controlled dissolution (Biswakarma et al. 2018).

In general, our results suggest that the catalytic effect of Fe(II) on ligand-controlled dissolution may enhance dissolution rates of Fe(III) (hydr)oxide minerals under a wide range of environmental conditions and we expect that it may have broad relevance in soil and aquatic environments.

Acknowledgments

We thank Herwig Lenitz for his assistance with the ICP-MS measurements and Gabriel Sigmund for his help with the BET-analysis. This work was supported by the Austrian Science Fund (FWF, grant no. I1528-N19 and I2865-N34). JB, SB, JH and SH were supported by the Swiss National Science Foundation (Project number 200021L_150150).

Supporting Information Available

The Supporting Information is available free of charge via the Internet at http://pubs.acs.org/ and contains adsorption isotherm data, a description of the procedure for calculating dissolution rates and adsorbed Fe(II) concentrations, an overview of the materials used, a summary of the batch dissolution experiments and dissolution rates, Fe(II) speciation modelling results and an overview of dissolution rates and the catalytic effect of Fe(II) as a function of pH, in 7 Figures and 4 Tables.

References

1. Kraemer, S. M.; Crowley, D. E.; Kretzschmar, R., Geochemical aspects of phytosiderophore-promoted iron acquisition by plants. In *Advances in Agronomy, Vol 91*, Sparks, D. L., Ed. Elsevier Academic Press Inc: San Diego, 2006; Vol. 91, pp 1-46.
2. Zinder, B.; Furrer, G.; Stumm, W., The coordination chemistry of weathering. 2.Dissolution of Fe(III)oxides *Geochim. Cosmochim. Acta* **1986,** *50*, (9), 1861-1869.
3. Cornell, R. M., ; Schwermann, U, *The Iron Oxides: Structure, Properties, Reactions, Occurrences and Uses*. Wiley: New York, 2003.
4. Tamura, H.; Kawamura, S.; Hagayama, M., Acceleration of the oxidation of Fe2+ ions by Fe(III)-oxyhydroxides. *Corrosion Sci.* **1980,** *20*, (8-9), 963-971.
5. Jones, A. M.; Griffin, P. J.; Collins, R. N.; Waite, T. D., Ferrous iron oxidation under acidic conditions - The effect of ferric oxide surfaces (vol 140, pg 1, 2014). *Geochim. Cosmochim. Acta* **2015,** *156*, 241-241.
6. Suzuki, Y.; Kuma, K.; Kudo, I.; Hasebe, K.; Matsunaga, K., Existence of stable Fe(II) complex in oxic river water and its determination *Water Res.* **1992,** *26*, (11), 1421-1424.
7. Nowack, B.; Sigg, L., Dissolution of Fe(III)(hydr)oxides by metal-EDTA complexes. *Geochim. Cosmochim. Acta* **1997,** *61*, (5), 951-963.
8. Bondietti, G.; Sinniger, J.; Stumm, W., The reactivity of Fe(III)(hydr)xodies - Effects of ligands in inhibiting the dissolution. *Colloid Surf. A-Physicochem. Eng. Asp.* **1993,** *79*, (2-3), 157-167.
9. Stumm, W. F., G.; Wieland, E.; Zinder, E., *The Effects of Complex-Forming Ligands on the Dissolution of Oxides and Aluminosilicates*. The chemistry of weathering: Netherland, 1985.
10. Stumm, W., Reactivity at the mineral-water interface: Dissolution and inhibition. *Colloid Surf. A-Physicochem. Eng. Asp.* **1997,** *120*, (1-3), 143-166.
11. Reichard, P. U.; Kretzschmar, R.; Kraemer, S. M., Dissolution mechanisms of goethite in the presence of siderophores and organic acids. *Geochim. Cosmochim. Acta* **2007,** *71*, (23), 5635-5650.
12. Kraemer, S. M., Iron oxide dissolution and solubility in the presence of siderophores. *Aquat. Sci.* **2004,** *66*, (1), 3-18.
13. Kuhn, K. M.; DuBois, J. L.; Maurice, P. A., Aerobic Microbial Fe Acquisition from Ferrihydrite Nanoparticles: Effects of Crystalline Order, Siderophores, and Alginate. *Environ. Sci. Technol.* **2014,** *48*, (15), 8664-8670.
14. Martin-Fernandez, C.; Lopez-Rayo, S.; Hernandez-Apaolaza, L.; Lucena, J. J., Timing for a sustainable fertilisation of Glycine max by using HBED/Fe3+ and EDDHA/Fe3+ chelates. *J. Sci. Food Agric.* **2017,** *97*, (9), 2773-2781.
15. Zinder, B.; Furrer, G.; Stumm, W., The coordination chemistry of weathering. 2. Dissolution of Fe(III)oxide *Geochim. Cosmochim. Acta* **1986,** *50*, (9), 1861-1869.
16. Wiederhold, J. G.; Kraemer, S. M.; Teutsch, N.; Borer, P. M.; Halliday, A. N.; Kretzschmar, R., Iron isotope fractionation during proton-promoted, ligand-controlled, and reductive dissolution of goethite. *Environ. Sci. Technol.* **2006,** *40*, (12), 3787-3793.
17. Suter, D.; Banwart, S.; Stumm, W., Dissolution of hydrous iron(III) oxides by reductive mechanisms. *Langmuir* **1991,** *7*, (4), 809-813.

18. Vartivarian, S. E.; Cowart, R. E., Extracellular iron reductases: Identification of a new class of enzymes by siderophore-producing microorganisms. *Arch. Biochem. Biophys.* **1999,** *364*, (1), 75-82.

19. Tomasi, N.; Weisskopf, L.; Renella, G.; Landi, L.; Pinton, R.; Varanini, Z.; Nannipieri, P.; Torrent, J.; Martinoia, E.; Cesco, S., Flavonoids of white lupin roots participate in phosphorus mobilization from soil. *Soil Biol. Biochem.* **2008,** *40*, (7), 1971-1974.

20. Wang, Z. M.; Schenkeveld, W. D. C.; Kraemer, S. M.; Giammar, D. E., Synergistic Effect of Reductive and Ligand-Promoted Dissolution of Goethite. *Environ. Sci. Technol.* **2015,** *49*, (12), 7236-7244.

21. Schenkeveld, W. D. C.; Wang, Z. M.; Giammar, D. E.; Kraemer, S. M., Synergistic Effects between Biogenic Ligands and a Reductant in Fe Acquisition from Calcareous Soil. *Environ. Sci. Technol.* **2016,** *50*, (12), 6381-6388.

22. Banwart, S.; Davies, S.; Stumm, W., The role of oxalate in accelerating the reductive dissolution of hematite (alpha-Fe2O3) by ascorbate. *Colloids and Surfaces* **1989,** *39*, (4), 303-309.

23. Yanina, S. V.; Rosso, K. M., Linked reactivity at mineral-water interfaces through bulk crystal conduction. *Science* **2008,** *320*, (5873), 218-222.

24. Gorski, C. A.; Edwards, R.; Sander, M.; Hofstetter, T. B.; Stewart, S. M., Thermodynamic Characterization of Iron Oxide-Aqueous Fe2+ Redox Couples. *Environ. Sci. Technol.* **2016,** *50*, (16), 8538-8547.

25. Williams, A. G. B.; Scherer, M. M., Spectroscopic evidence for Fe(II)-Fe(III) electron transfer at the iron oxide-water interface. *Environ. Sci. Technol.* **2004,** *38*, (18), 4782-4790.

26. Frierdich, A. J.; Helgeson, M.; Liu, C. S.; Wang, C. M.; Rosso, K. M.; Scherer, M. M., Iron Atom Exchange between Hematite and Aqueous Fe(II). *Environ. Sci. Technol.* **2015,** *49*, (14), 8479-8486.

27. Latta, D. E.; Gorski, C. A.; Scherer, M. M., Influence of Fe2+-catalysed iron oxide recrystallization on metal cycling. *Biochem. Soc. Trans.* **2012,** *40*, 1191-1197.

28. Hiemstra, T.; VanRiemsdijk, W. H., A surface structural approach to ion adsorption: The charge distribution (CD) model. *J. Colloid Interface Sci.* **1996,** *179*, (2), 488-508.

29. Sugimoto, T.; Sakata, K., Preparation of monodisperse pseudocubic alpha-Fe2O3 particles from condensed ferric hydroxide gel. *J. Colloid Interface Sci.* **1992,** *152*, (2), 587-590.

30. Schwertmann, U. C., R. M., *Iron Oxides in the Laboratory: Preparation and Characterization*. Second ed.; John Wiley & Sons: Germany, 2008.

31. Morup, S.; Madsen, M. B.; Franck, J.; Villadsen, J.; Koch, C. J. W., A new interpretation of mossbauer-spectra of microcrystalline goethite - Super-ferromagnetism or super-spin-glass behavior *J. Magn. Magn. Mater.* **1983,** *40*, (1-2), 163-174.

32. Schwertman, U.; Friedl, J. I.; Kyek, A., Formation and properties of a continuous crystallinity series of synthetic ferrihydrites (2-to 6-line) and their relation to FeOOH forms. *Clay Clay Min.* **2004,** *52*, (2), 221-226.

33. Pedersen, H. D.; Postma, D.; Jakobsen, R.; Larsen, O., Fast transformation of iron oxyhydroxides by the catalytic action of aqueous Fe(II). *Geochim. Cosmochim. Acta* **2005,** *69*, (16), 3967-3977.

34. Park, B.; Dempsey, B. A., Heterogeneous oxidation of Fe(II) on ferric oxide at neutral pH and a low partial pressure of 0(2). *Environ. Sci. Technol.* **2005,** *39*, (17), 6494-6500.

35. Mikutta, C.; Mikutta, R.; Bonneville, S.; Wagner, F.; Voegelin, A.; Christl, I.; Kretzschmar, R., Synthetic coprecipitates of exopolysaccharides and ferrihydrite. Part I: Characterization. *Geochim. Cosmochim. Acta* **2008,** *72*, (4), 1111-1127.

36. Mikutta, C.; Kretzschmar, R., Synthetic coprecipitates of exopolysaccharides and ferrihydrite. Part II: Siderophore-promoted dissolution. *Geochim. Cosmochim. Acta* **2008,** *72*, (4), 1128-1142.

37. Parkhurst, D. L. a. A., C. A. *Description of input and examples for PHREEQC Version 3 – a computer program for speciation, batch-reaction, onedimensional transport and inverse geochemical calculations.*; 2013; p 497.

38. Kim, D.; Duckworth, O. W.; Strathmann, T. J., Reactions of aqueous iron-DFOB (desferrioxamine B) complexes with flavin mononucleotide in the absence of strong iron(II) chelators. *Geochim. Cosmochim. Acta* **2010,** *74*, (5), 1513-1529.

39. Buchholz, A.; Laskov, C.; Haderlein, S. B., Effects of Zwitterionic Buffers on Sorption of Ferrous Iron at Goethite and Its Oxidation by CCl4. *Environ. Sci. Technol.* **2011,** *45*, (8), 3355-3360.

40. Furrer, G.; Stumm, W., The coordination chemistry of weathering: 1. dissolution kinetics of delta-Al2O3 and BeO. *Geochim. Cosmochim. Acta* **1986,** *50*, (9), 1847-1860.

41. Suter, D.; Siffert, C.; Sulzberger, B.; Stumm, W., Catalytic dissolution of iron(III)(hydr)oxides by oxalic-acid in the presence of Fe(II). *Naturwissenschaften* **1988,** *75*, (11), 571-573.

42. Biswakarma, J.; Kang, K.; Borowski, S. C.; Schenkeveld, W. D. C.; Kraemer, S. M.; Hering, J. G.; Hug, S. J., Fe(II)-catalyzed ligand-controlled dissolution of iron(hydr)oxides. *submitted to Environ. Sci. Technol. 2018.*

43. Borer, P.; Kraemer, S. M.; Sulzberger, B.; Hug, S. J.; Kretzschmar, R., Photodissolution of lepidocrocite (gamma-FeOOH) in the presence of desferrioxamine B and aerobactin. *Geochim. Cosmochim. Acta* **2009,** *73*, (16), 4673-4687.

44. Zhang, Y.; Charlet, L.; Schindler, P. W., Adsorption of protons, Fe(II) and Al(III) on lepidocrocite *Colloids and Surfaces* **1992,** *63*, (3-4), 259-268.

45. Hiemstra, T.; van Riemsdijk, W. H., Adsorption and surface oxidation of Fe(II) on metal (hydr)oxides. *Geochim. Cosmochim. Acta* **2007,** *71*, (24), 5913-5933.

46. Zhang, Y.; Charlet, L.; Schindler, P. W., Adsorption of protons, Fe(II) and Al(III) on lepidocrocite (gamma-FeOOH). *Colloids and Surfaces* **1992,** *63*, (3-4), 259-268.

47. Kozin, P. A.; Salazar-Alvarez, G.; Boily, J. F., Oriented Aggregation of Lepidocrocite and Impact on Surface Charge Development. *Langmuir* **2014,** *30*, (30), 9017-9021.

Main figures and table

Figure. 1. Dissolution of lepidocrocite by HBED and DFOB in the presence of various concentrations of Fe(II) and dissolution rates as a function of adsorbed Fe(II) concentration

Figure. 2. Dissolution of lepidocrocite by DFOB in the presence and absence of Fe(II) at various pH conditions

Figure. 3. Dissolution of various types of Fe(III) (hydr) oxide mineral by ligand in the presence and absence of Fe(II)

Table. 1. Comparison of dissolution rates, the size of catalytic effect of Fe(II) and rate coefficients between various types of Fe(III) (hydr) oxide mineral

TOC figure

Figure 1. Fe mobilization from lepidocrocite (0.1 g L^{-1}, 0.01 M NaCl) by (a) 20 µM DFOB and (c) 17.6 µM HBED as a function of time for various applied Fe(II) concentrations at pH 6. Error bars indicate standard deviations. Lepidocrocite dissolution rates for (b) Fe(II) + DFOB and (d) Fe(II) + HBED as a function of the adsorbed Fe(II) concentration (uncorrected for ligand adsorption). Adsorbed Fe(II) concentrations at t=0 were calculated based on adsorption isotherm (SI. Fig. 1 (a), SI. Fig. 5). Dissolution rates were calculated from the slopes of linear regression lines over the time interval t = 0.5 -2 h for the treatments presented in panel (a) and (c). The calculation procedure is described in the SI. Fig.4.

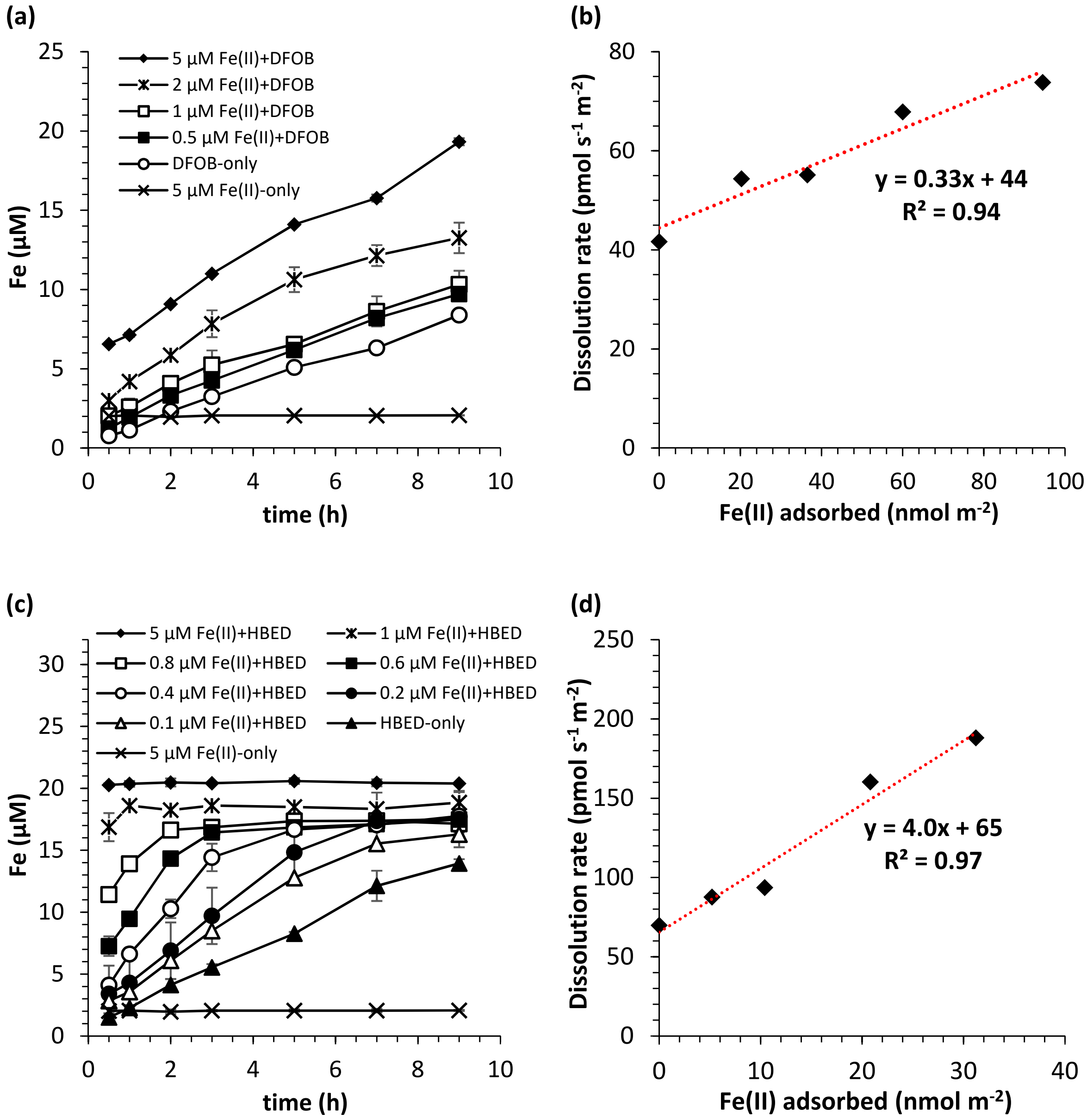

Figure 2. Fe mobilization from lepidocrocite (0.1 g L^{-1}, 0.01 M NaCl) by 20 µM DFOB as a function of time in presence and absence of 5 µM Fe(II) at (a) pH 4, (b) pH 6, (c) pH 7 and (d) pH 8.5. Error bars indicate standard deviations. 5 µM Fe(II) was added in two different ways; Fe(II)(20 min earlier)+DFOB: Fe(II) was added 20 min before the ligand was added, Fe(II)+DFOB: Fe(II) and DFOB were added at the same time by adding pre-mixed Fe(II) and DFOB stock solution.

(a) - pH 4 **(b) - pH 6**

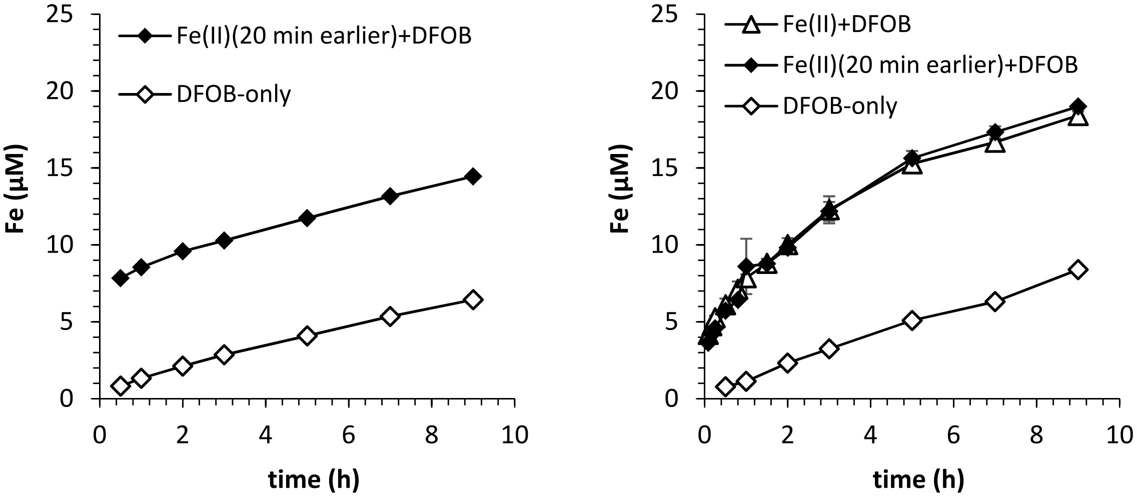

(c) - pH 7 **(d) - pH 8.5**

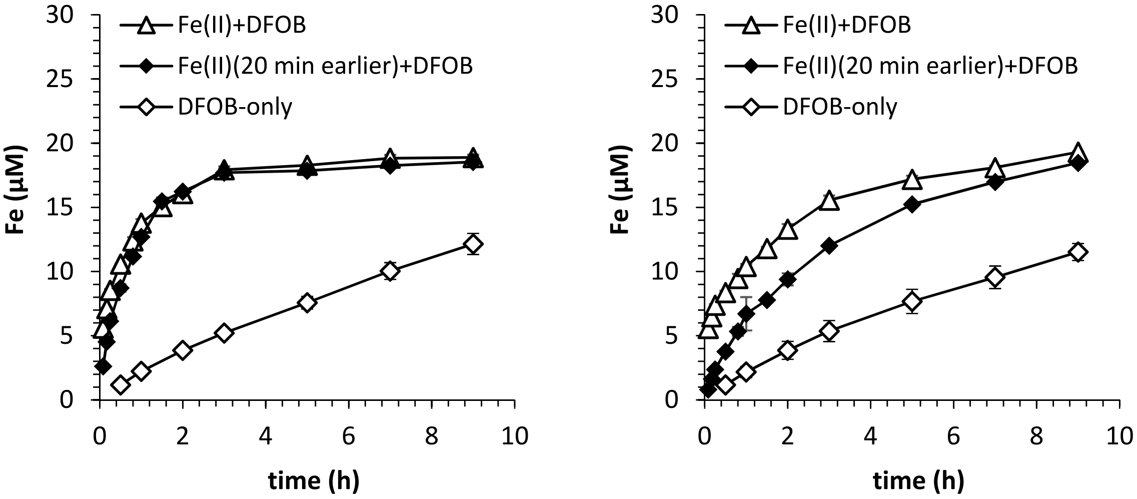

Figure 3. Fe mobilization from (a-b) hematite, (c-d) goethite-2, (e-f) goethite-1, and (g-h) 2-line ferrihydrite and by 20 µM DFOB or 17.6 µM HBED and (i) lepidocrocite (0.1 g L^{-1}, 0.01 M NaCl) by 20 µM DFOB in the presence and absence of Fe(II) (2 µM for DFOB and 1 µM for HBED) as a function of time at a fixed pH (pH 7 for DFOB and pH 6 for HBED). The unit of time on the x-axis is hours (h) for hematite and goethite (a-f) and minutes (min) for 2-line ferrihydrite and lepidocrocite (g-i). Error bars indicate standard deviations.

(a) - hematite, DFOB **(b) - hematite, HBED**

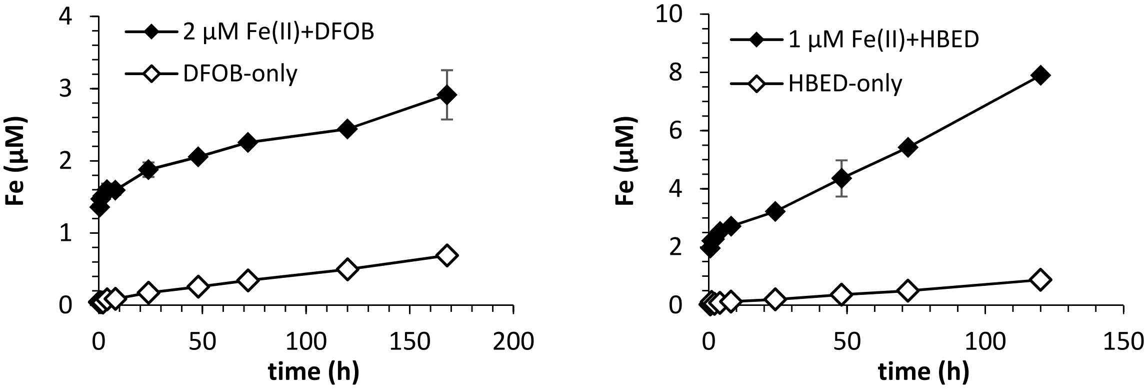

(c) - goethite-2, DFOB **(d) - goethite-2, HBED**

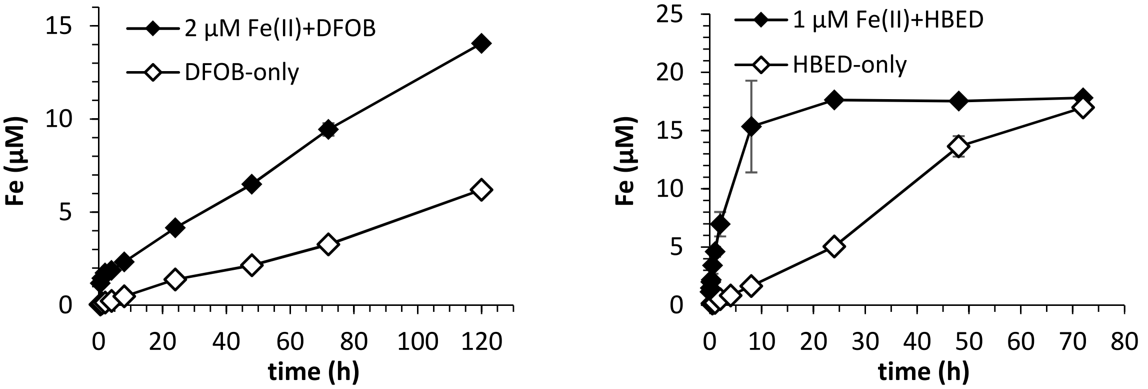

(e) - goethite-1, DFOB **(f) - goethite-1, HBED**

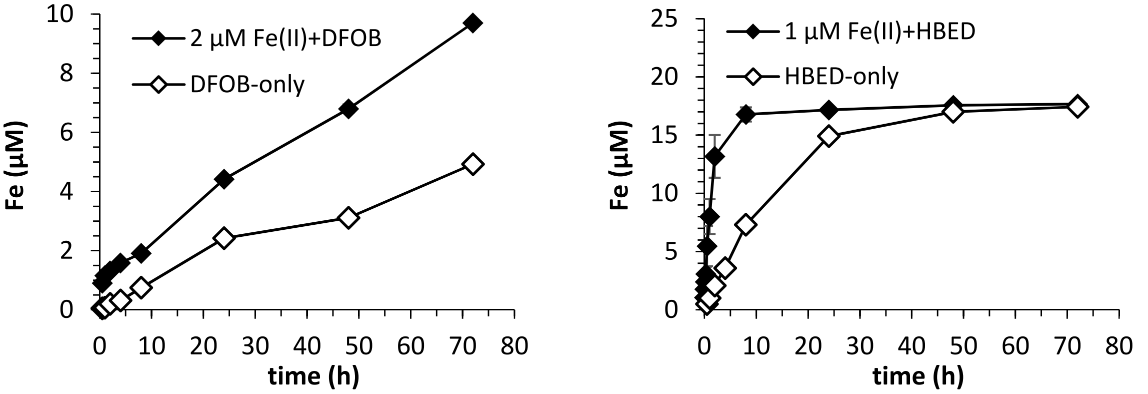

(g)- 2-line ferrihydrite, DFOB

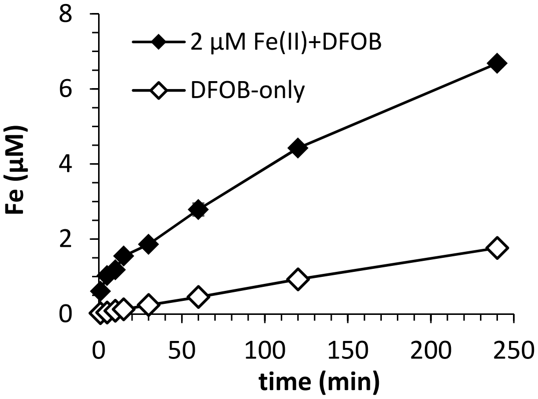

(h) - 2-line ferrihydrite, HBED

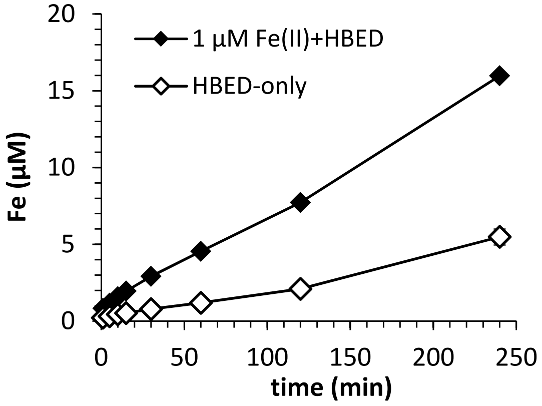

(i) - lepidocrocite, DFOB

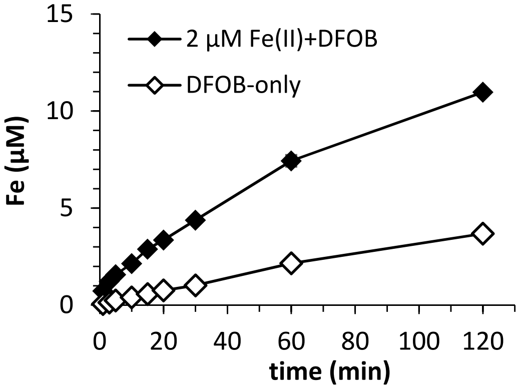

Table 1. Dissolution rates, catalytic effect of Fe(II) (C. E. Fe(II)) and rate coefficients for various Fe(III) (hydr) oxide minerals. The catalytic effect of Fe(II) is the ratio between the dissolution rates in the treatment with both Fe(II) and ligands (R_{net}) and the treatment with ligands only (R_L). Rate coefficients of ligand-controlled dissolution (k_L) and Fe(II) catalyzed ligand-controlled dissolution ($k_{(Fe(II))}$) were determined according to rate law equations (3, 4) using the adsorbed Fe(II) ($Fe(II)_{ads}$) and HBED ($HBED_{ads}$) concentrations. No rate coefficients were determined for 2-line ferrihydrite since no surface area normalized net dissolution rates were available.

Fe(III) (hydr) oxide	treatment	R_L (pmol s^{-1} m^{-2})	R_{net} (pmol s^{-1} m^{-2})	C. E. Fe(II)	$Fe(II)_{ad}$ (µmol m^{-2})	$HBED_{ads}$ (µmol m^{-2})	k_{HBED} (s^{-1})	$k_{Fe(II)}$ (HBED) (µmol^{-1} m^2 s^{-1})
hematite	2 µM Fe(II) + DFOB		9.5×10^{-1}	2.1				
	DFOB-only	4.5×10^{-1}						
	1 µM Fe(II) + HBED		5.9	6.9	1.8×10^{-2}	1.2×10^{-1}		2.3×10^{-3}
	HBED -only	8.5×10^{-1}					7.2×10^{-6}	
goethite-2	2 µM Fe(II) + DFOB		9.2	2.1				
	DFOB-only	4.3						
	1 µM Fe(II) + HBED		2.3×10^{2}	13	2.2×10^{-2}	0.9×10^{-1}		1.1×10^{-1}
	HBED -only	18					2.0×10^{-4}	
goethite-1	2 µM Fe(II) + DFOB		3.2	1.8				
	DFOB-only	1.8						
	1 µM Fe(II) + HBED		1.9×10^{2}	7.9	3.3×10^{-2}	0.6×10^{-1}		7.9×10^{-2}
	HBED -only	24					3.8×10^{-4}	
lepidocrocite	2 µM Fe(II) + DFOB		2.9×10^{2}	4				
	DFOB-only	73						
	0.1 µM Fe(II) + HBED		88	1.3	0.5×10^{-2}	1.7×10^{-1}		[a]1.8×10^{-2} (SD: 6.0×10^{-3})
	0.2 µM Fe(II) + HBED		94	1.3	1.0×10^{-2}			
	0.4 µM Fe(II) + HBED		1.6×10^{2}	2.3	2.1×10^{-2}			
	0.6 µM Fe(II) + HBED		1.9×10^{2}	2.7	3.1×10^{-2}			
	HBED -only	70					4.2×10^{-4}	
2-line ferrihydrite	2 µM Fe(II) + DFOB		[b]4.9×10^{3}	4.1				
	DFOB-only	[b]1.2×10^{3}						
	1 µM Fe(II) + HBED		[b]1.0×10^{4}	3				
	HBED -only	[b]3.4×10^{3}						

All experiments have been performed with 0.1 g L^{-1} Fe(III) (hydr)oxide (0.01 M NaCl). The experiments involving DFOB were performed at a ligand concentration of 20 µM at pH 7 and the experiments involving HBED were performed at a ligand concentration of 17.6 µM at pH 6.

[a] Average rate coefficients and standard deviation (SD) based on observations in the presence of 0.1 to 0.6 µM of Fe(II).

[b] The unit of dissolution rates for 2-line ferrihydrite is **pmol s^{-1} g^{-1}** (normalized per mass (g), not per surface area), because the ligand-accessible specific surface area could not be determined by BET analysis for 2-line ferrihydrite.

Graphical Abstract / TOC abstract

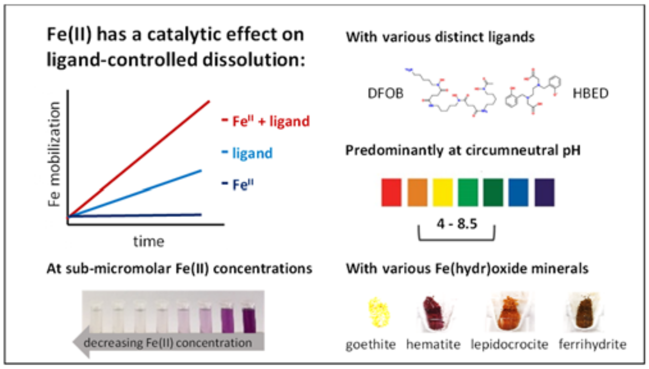
Fe(II) has a catalytic effect on ligand-controlled dissolution:
Fe mobilization
time
Fe^II + ligand
ligand
Fe^II
At sub-micromolar Fe(II) concentrations
decreasing Fe(II) concentration
With various distinct ligands
DFOB
HBED
Predominantly at circumneutral pH
4 - 8.5
With various Fe(hydr)oxide minerals
goethite
hematite
lepidocrocite
ferrihydrite